Progress Toward Understanding the Resistive Switching Process in RRAM Devices

Blanka Magyari-Köpe and Yoshio Nishi

Students: **Liang Zhao**
Dan Duncan
Seong-Geon Park (Samsung)
Hyung-Dong Lee (Hynix)

RRAM as Emerging Memory

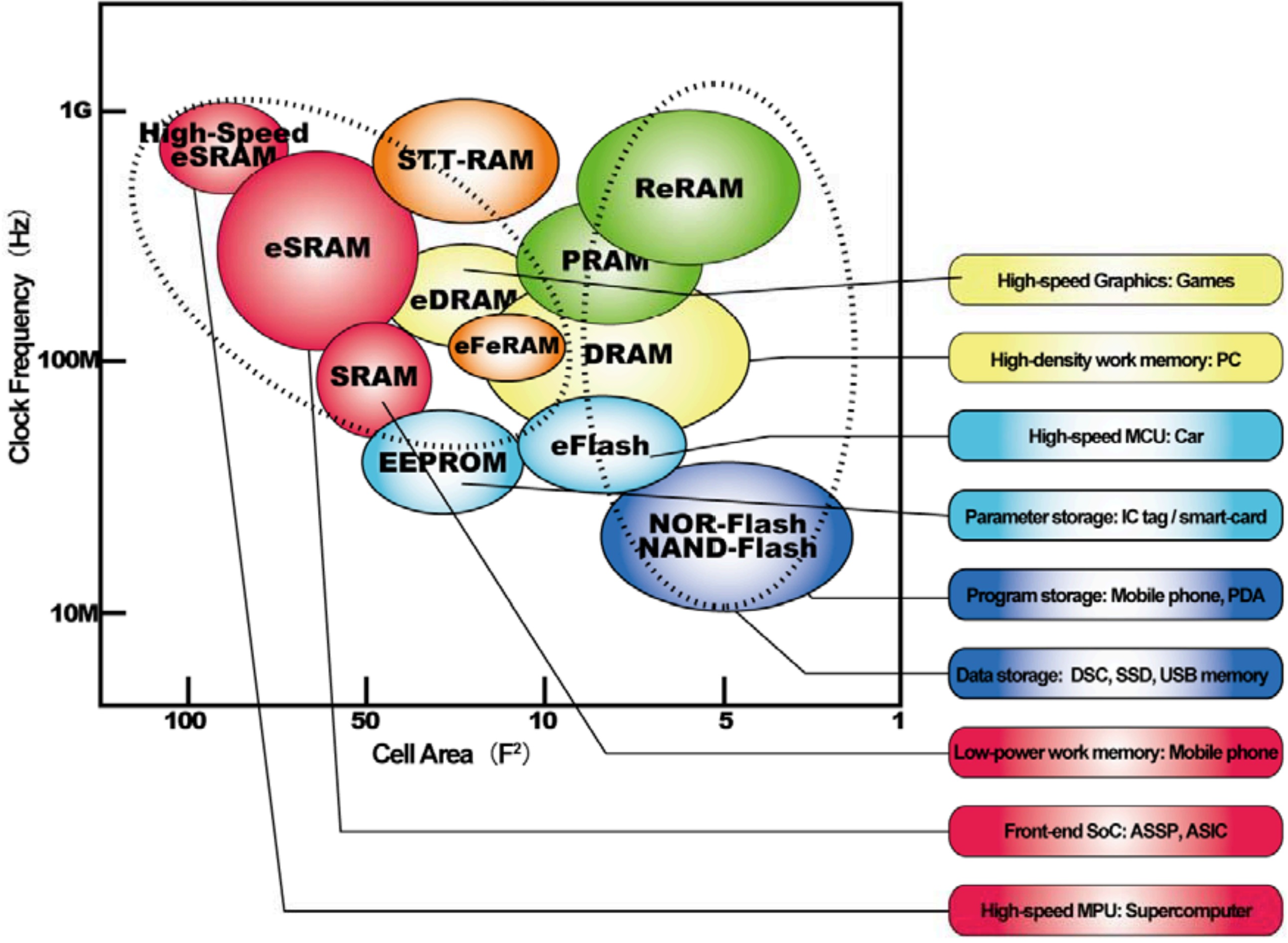
Role-sharing Positioning of Emerging Research Memories

Web of Science Citations for RRAM and ReRAM

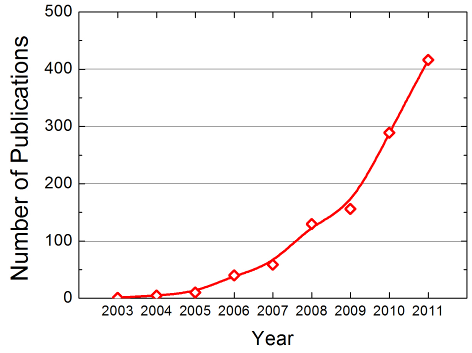

H. Akinaga, AIST, Maturity Evaluation for Selected Emerging Research Memory Technologies, 2010.

Metal Oxide M-I-M Memory (RRAM)

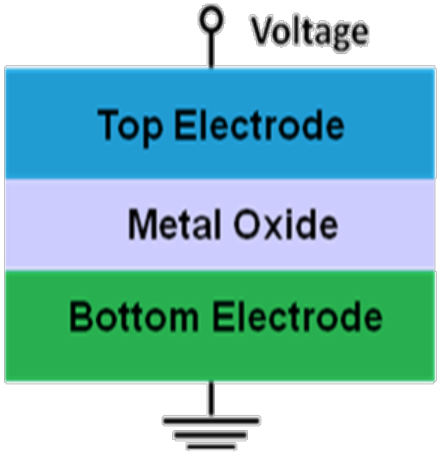

- **Motivation:**
  - Low programming voltage (< 3V)
  - Material set compatible with conventional semiconductor processing (e.g Ni, Hf, Al…)
  - Low temperature processing (BEOL-compatible)
  - High speed and density
  - Structural simplicity

- **Key issues:**
  - Physics of resistive switching
  - Device scaling properties
  - Device uniformity

Flash Memory

RRAM Materials Choices

The Periodic Table of the Elements

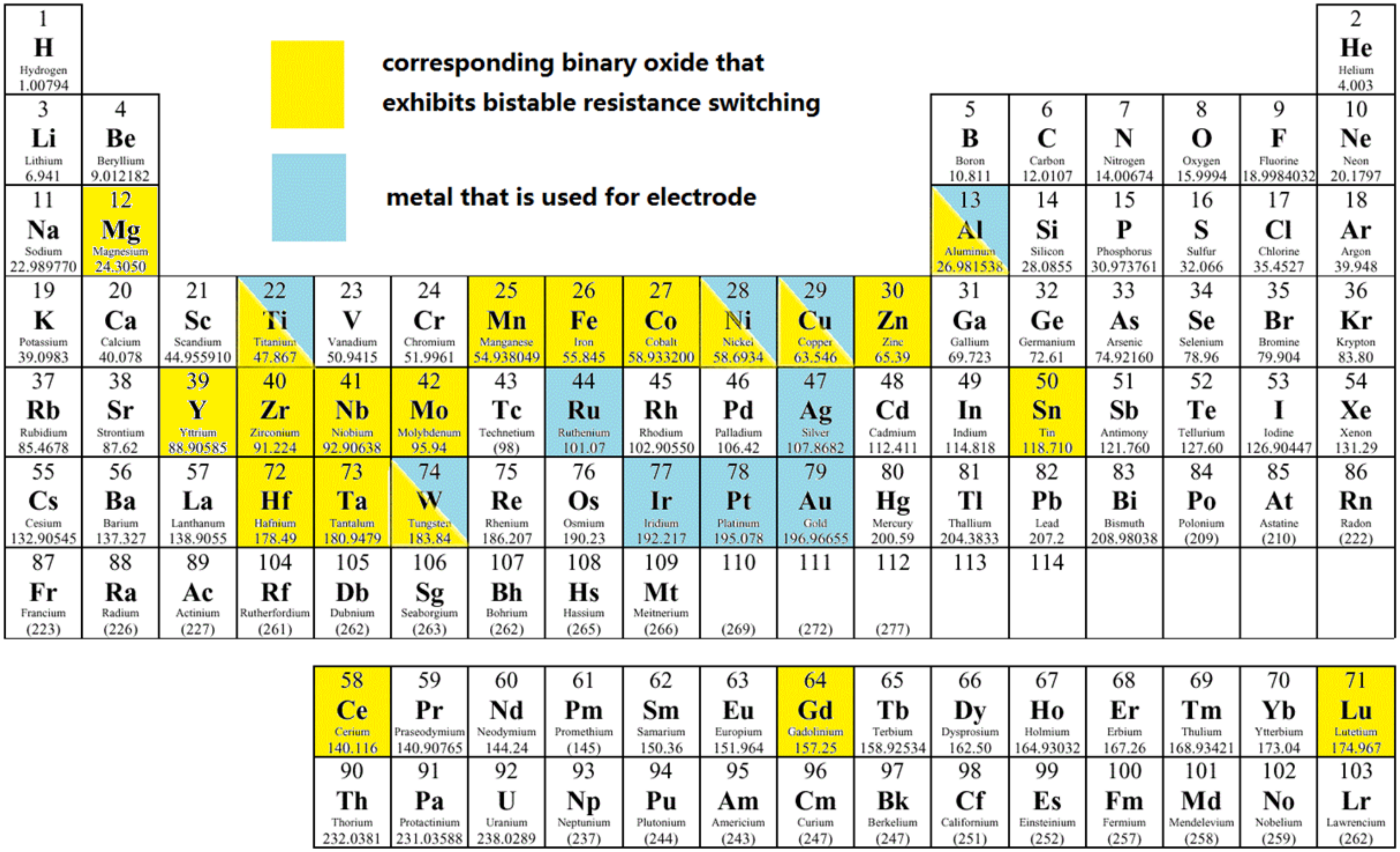

🟨 corresponding binary oxide that exhibits bistable resistance switching

🟦 metal that is used for electrode

1 H Hydrogen 1.00794																	2 He Helium 4.003
3 Li Lithium 6.941	4 Be Beryllium 9.012182											5 B Boron 10.811	6 C Carbon 12.0107	7 N Nitrogen 14.00674	8 O Oxygen 15.9994	9 F Fluorine 18.9984032	10 Ne Neon 20.1797
11 Na Sodium 22.989770	12 Mg Magnesium 24.3050											13 Al Aluminum 26.981538	14 Si Silicon 28.0855	15 P Phosphorus 30.973761	16 S Sulfur 32.066	17 Cl Chlorine 35.4527	18 Ar Argon 39.948
19 K Potassium 39.0983	20 Ca Calcium 40.078	21 Sc Scandium 44.955910	22 Ti Titanium 47.867	23 V Vanadium 50.9415	24 Cr Chromium 51.9961	25 Mn Manganese 54.938049	26 Fe Iron 55.845	27 Co Cobalt 58.933200	28 Ni Nickel 58.6934	29 Cu Copper 63.546	30 Zn Zinc 65.39	31 Ga Gallium 69.723	32 Ge Germanium 72.61	33 As Arsenic 74.92160	34 Se Selenium 78.96	35 Br Bromine 79.904	36 Kr Krypton 83.80
37 Rb Rubidium 85.4678	38 Sr Strontium 87.62	39 Y Yttrium 88.90585	40 Zr Zirconium 91.224	41 Nb Niobium 92.90638	42 Mo Molybdenum 95.94	43 Tc Technetium (98)	44 Ru Ruthenium 101.07	45 Rh Rhodium 102.90550	46 Pd Palladium 106.42	47 Ag Silver 107.8682	48 Cd Cadmium 112.411	49 In Indium 114.818	50 Sn Tin 118.710	51 Sb Antimony 121.760	52 Te Tellurium 127.60	53 I Iodine 126.90447	54 Xe Xenon 131.29
55 Cs Cesium 132.90545	56 Ba Barium 137.327	57 La Lanthanum 138.9055	72 Hf Hafnium 178.49	73 Ta Tantalum 180.9479	74 W Tungsten 183.84	75 Re Rhenium 186.207	76 Os Osmium 190.23	77 Ir Iridium 192.217	78 Pt Platinum 195.078	79 Au Gold 196.96655	80 Hg Mercury 200.59	81 Tl Thallium 204.3833	82 Pb Lead 207.2	83 Bi Bismuth 208.98038	84 Po Polonium (209)	85 At Astatine (210)	86 Rn Radon (222)
87 Fr Francium (223)	88 Ra Radium (226)	89 Ac Actinium (227)	104 Rf Rutherfordium (261)	105 Db Dubnium (262)	106 Sg Seaborgium (263)	107 Bh Bohrium (262)	108 Hs Hassium (265)	109 Mt Meitnerium (266)	110 (269)	111 (272)	112 (277)	113	114				
				58 Ce Cerium 140.116	59 Pr Praseodymium 140.90765	60 Nd Neodymium 144.24	61 Pm Promethium (145)	62 Sm Samarium 150.36	63 Eu Europium 151.964	64 Gd Gadolinium 157.25	65 Tb Terbium 158.92534	66 Dy Dysprosium 162.50	67 Ho Holmium 164.93032	68 Er Erbium 167.26	69 Tm Thulium 168.93421	70 Yb Ytterbium 173.04	71 Lu Lutetium 174.967
				90 Th Thorium 232.0381	91 Pa Protactinium 231.03588	92 U Uranium 238.0289	93 Np Neptunium (237)	94 Pu Plutonium (244)	95 Am Americium (243)	96 Cm Curium (247)	97 Bk Berkelium (247)	98 Cf Californium (251)	99 Es Einsteinium (252)	100 Fm Fermium (257)	101 Md Mendelevium (258)	102 No Nobelium (259)	103 Lr Lawrencium (262)

Unipolar and/or Bipolar Switching

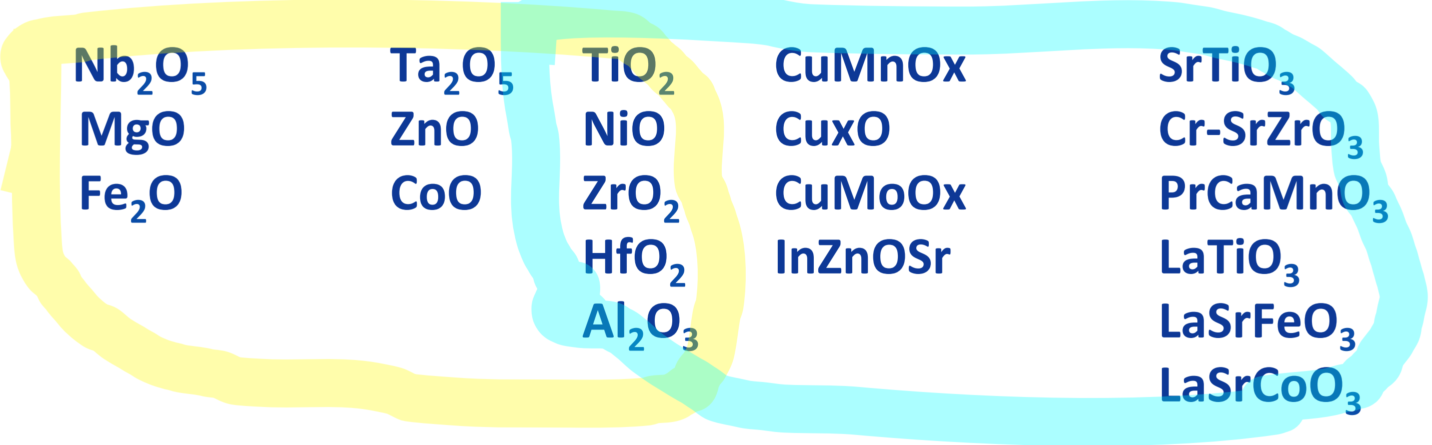

Transition metal oxides

Nb_2O_5
MgO
Fe_2O

Ta_2O_5
ZnO
CoO

TiO_2
NiO
ZrO_2
HfO_2
Al_2O_3

CuMnOx
CuxO
CuMoOx
InZnOSr

Perovskites

$SrTiO_3$
$Cr\text{-}SrZrO_3$
$PrCaMnO_3$
$LaTiO_3$
$LaSrFeO_3$
$LaSrCoO_3$

Unipolar

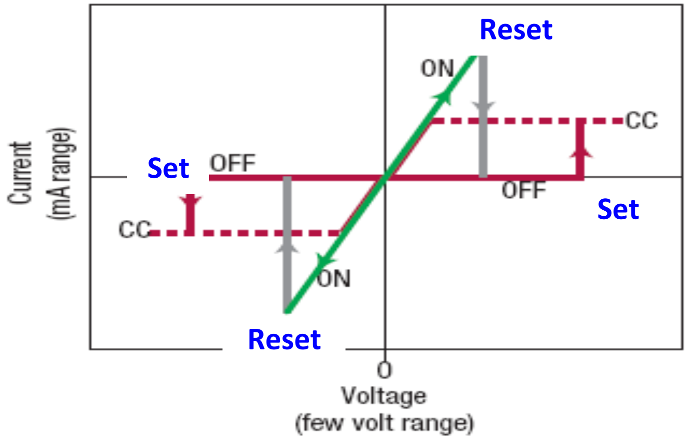

Bipolar

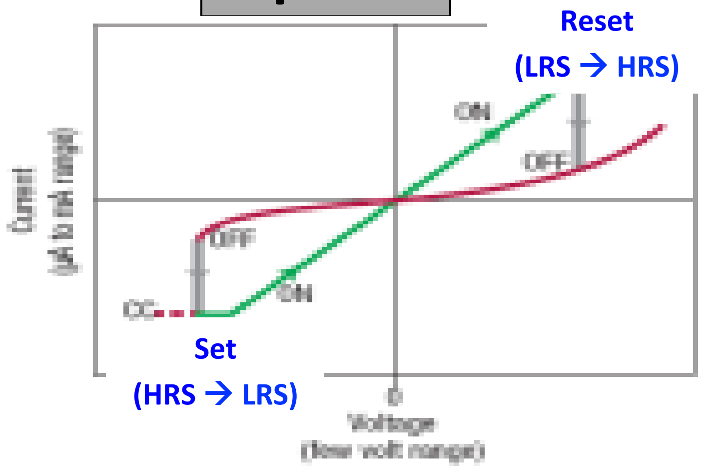

Forming and Switching Mechanisms

Forming

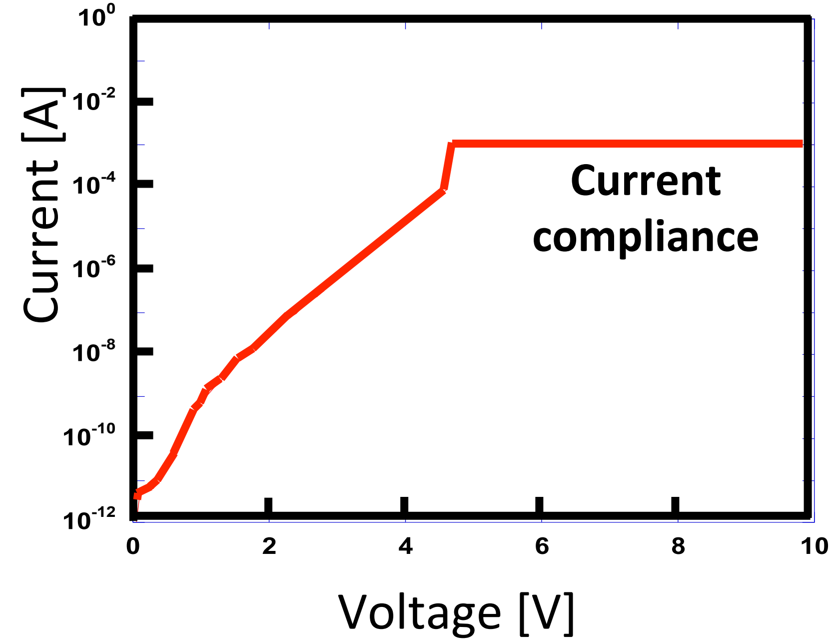

Switching

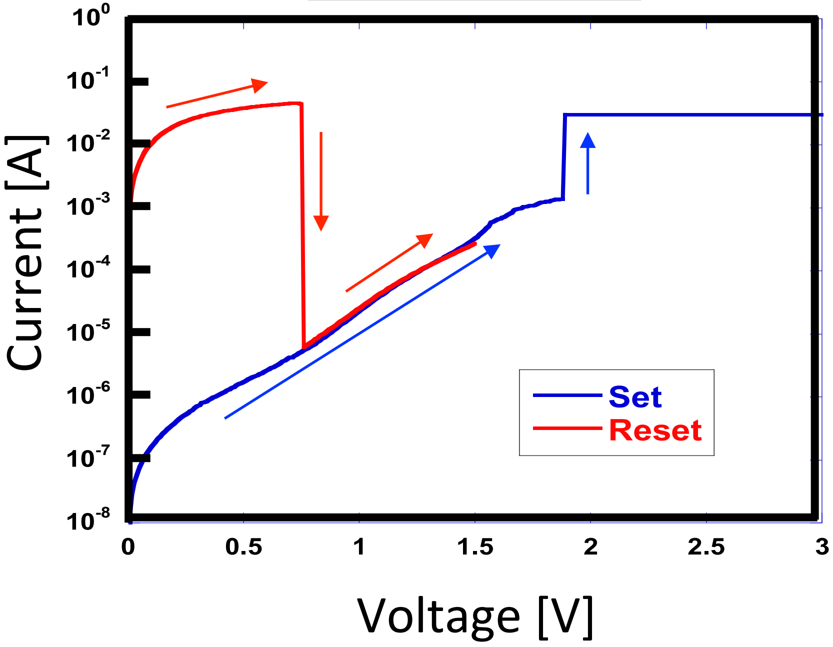

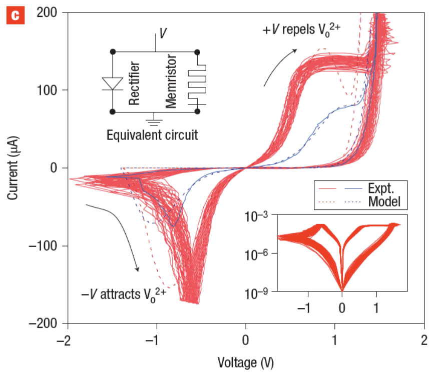

K. Tsunoda et al, Applied Physics Letters 90, 2007.
Strukov et al., Nature 453, 80, 2008.
Yang et al., Nature Nanotechnology 3, 429, 2008.

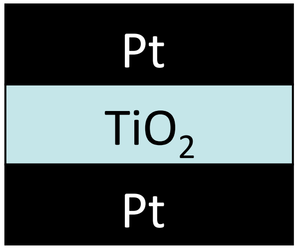

Pt

TiO_2

Pt

Models for Resistive Switching

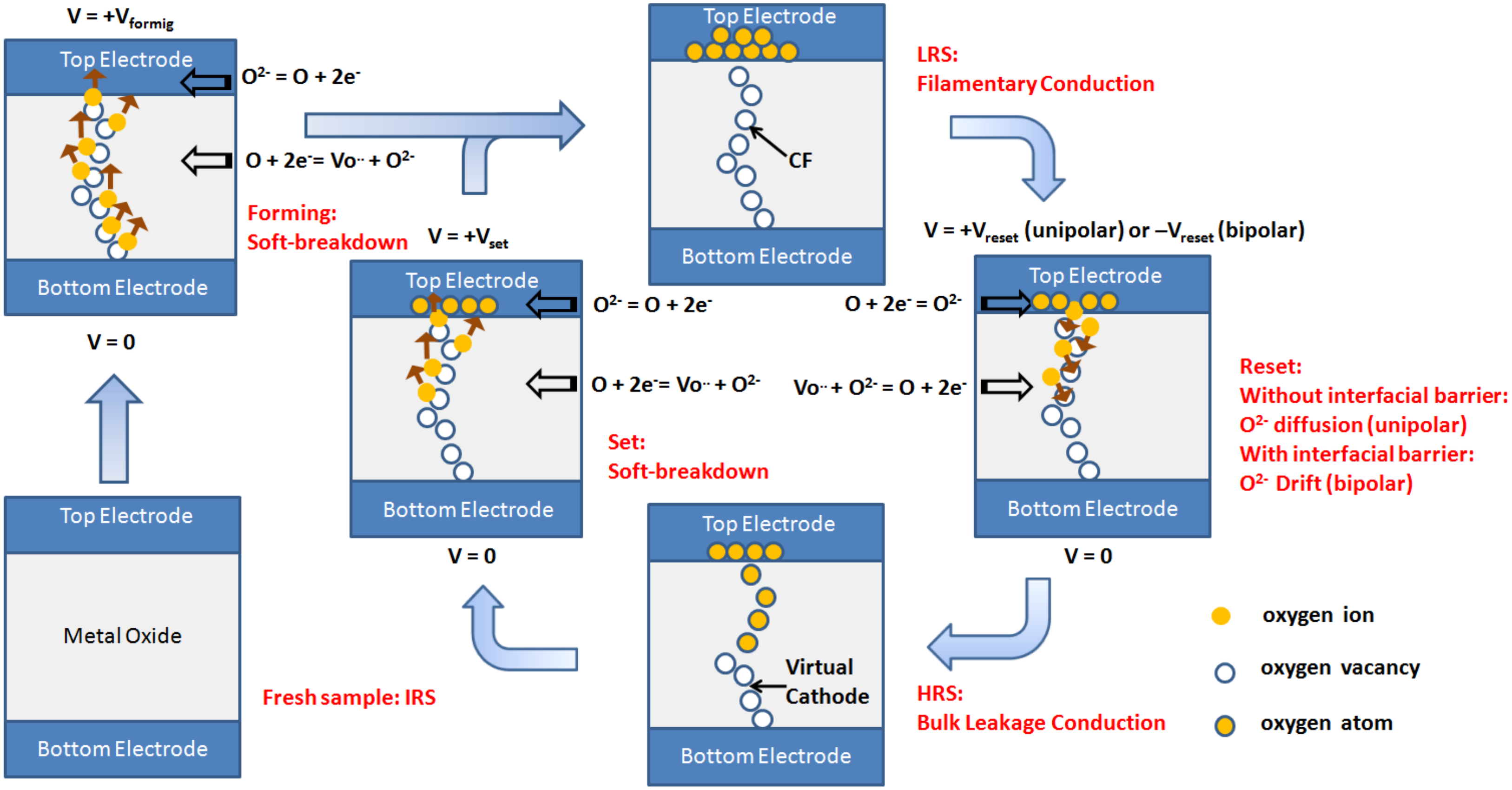

$V = +V_{formig}$

$O^{2-} = O + 2e^-$

$O + 2e^- = V_o^{\cdot\cdot} + O^{2-}$

Forming:
Soft-breakdown

$V = 0$

Fresh sample: IRS

LRS:
Filamentary Conduction

$V = +V_{set}$

$O^{2-} = O + 2e^-$

$O + 2e^- = V_o^{\cdot\cdot} + O^{2-}$

Set:
Soft-breakdown

$V = 0$

$V = +V_{reset}$ (unipolar) or $-V_{reset}$ (bipolar)

$O + 2e^- = O^{2-}$

$V_o^{\cdot\cdot} + O^{2-} = O + 2e^-$

Reset:
Without interfacial barrier:
O^{2-} diffusion (unipolar)
With interfacial barrier:
O^{2-} Drift (bipolar)

$V = 0$

HRS:
Bulk Leakage Conduction

● oxygen ion
○ oxygen vacancy
● oxygen atom

S. Yu, B. Lee, H.-S. P. Wong, "Metal Oxide Memory," in J. Wu, W. Han, H.-C. Kim, A. Janotti eds, "Functional Metal Oxide Nanostructures," Springer 2011.

Evidence of Oxygen Vacancy Filaments in Transition Metal Oxides

D.-H. Kwon et al., Nat. Nanotech., 5, 148-153, 2010

Oxygen gas after the electroforming process

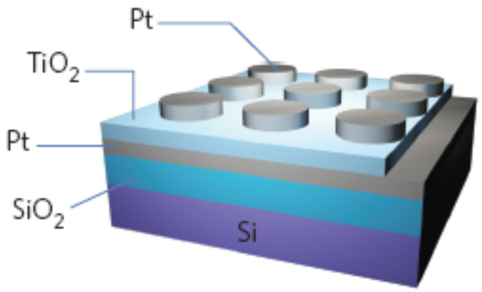

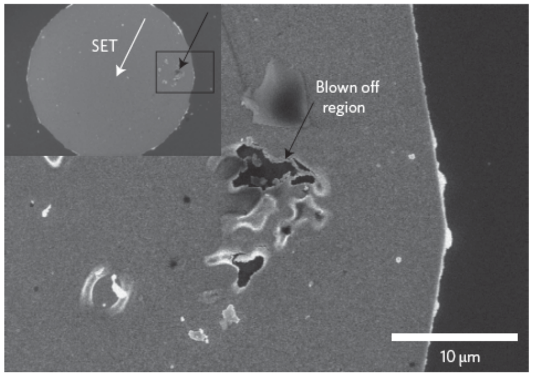

D.S. Jeong et al., *J. Appl. Phys*. 104, 123716, 2008.

Observation of oxygen gases in TiO_2 by TOF-SIMS

Janousch et al., Adv. Mat. 19, 2232 (2007)

V_o conducting path of Pt / $Cr:SrTiO_3$ / Pt devices

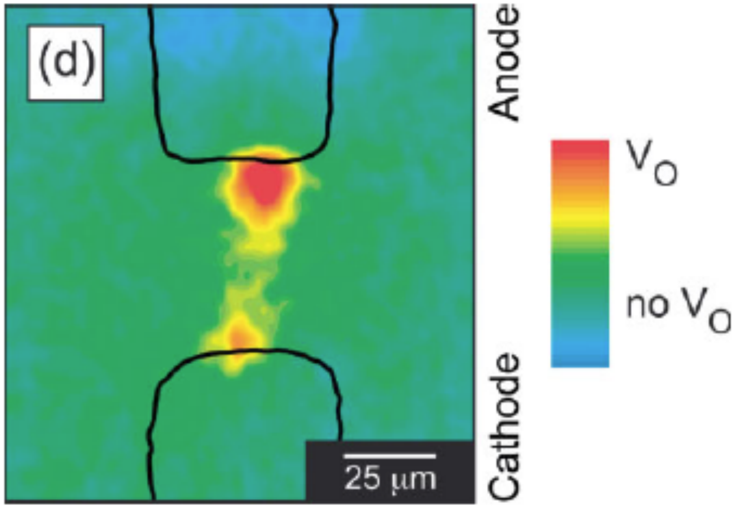

- **What is the role of oxygen vacancies on the on-state conduction and resistance switching mechanism?**

Nano-Filament Formation in Pt/TiO_2/Pt

X-ray absorption spectromicroscopy and TEM

J.P. Strachan et al., Adv. Mat. 22, 2010.

HRTEM and electron diffraction analysis

D.-H. Kwon et al., Nat. Nanotech., 5, 148-153, 2010.

•In-situ local I-V in TEM using conductive-AFM (C-AFM)

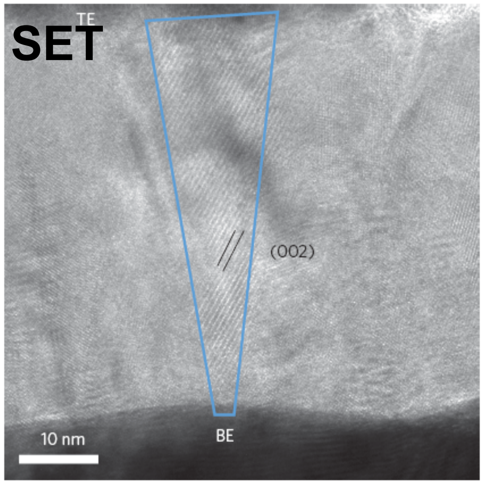

SET

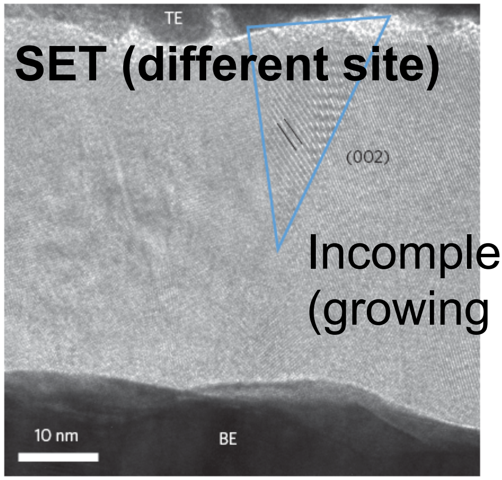

SET (different site)

Incomplete filament
(growing from TE)

- **A different phase with conical shape was observed after SET process.**
- **5~10nm diameter Magnéli phase (Ti_nO_{2n-1}) is confirmed by electron diffraction measurements .**

Ab initio Modeling of Switching Mechanisms

- **Metallic/semiconducting filament?**
- **Vacancy chain/filament - formation energy of conductive paths?**
- **Local density of states arising from vacancy distribution - metallic behavior?**
- **Transport, electronic or ionic?**
- **Macroscopic model vs atomic scale model?**

TiO$_2$: Single Vacancy Bulk Defects States

DOS (Density of States)

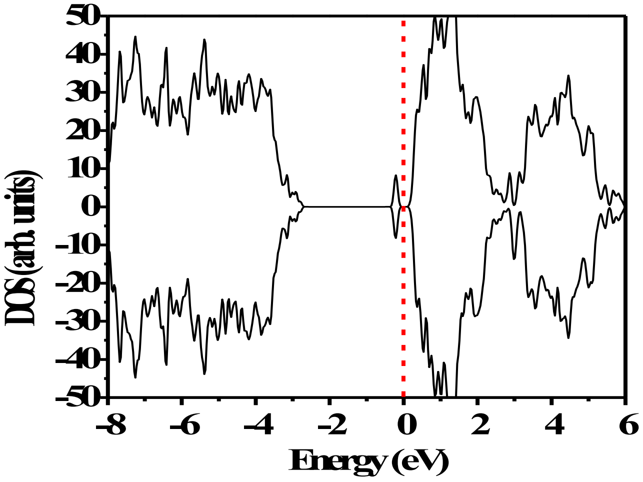

ELF (Electron Localization Function)

Bulk-like states for NN Ti

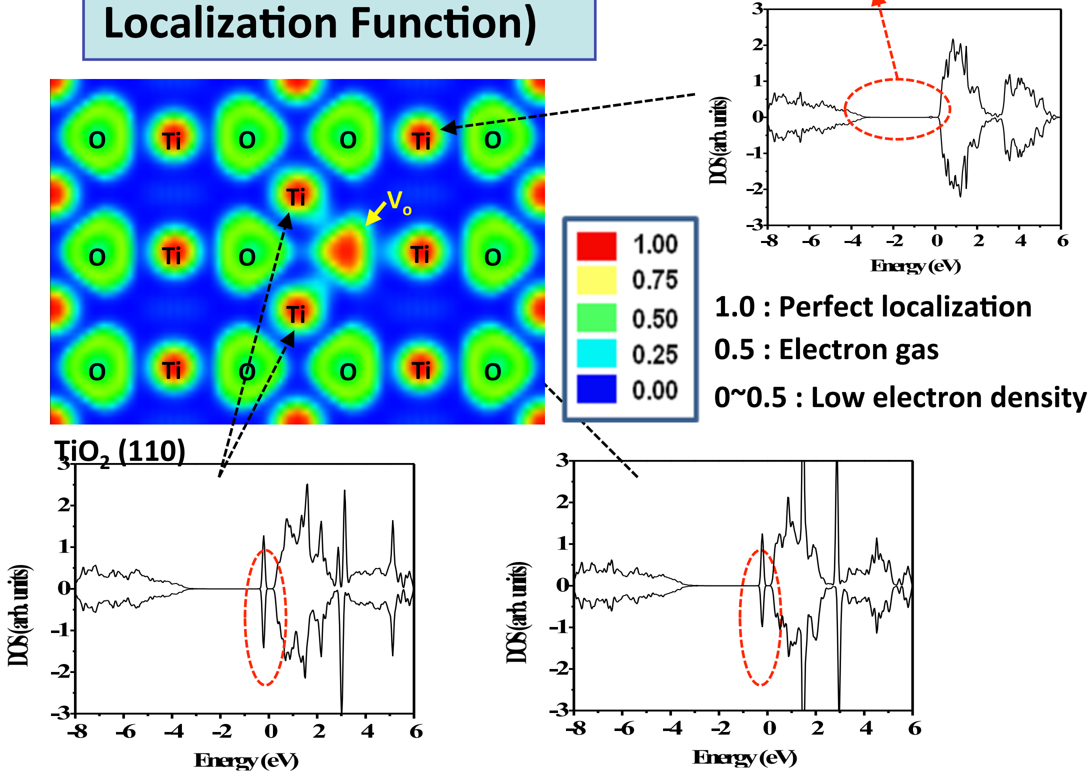

1.0 : Perfect localization

0.5 : Electron gas

0~0.5 : Low electron density

- Defect states are observed around ~ 0.4 eV below CBM.
- Electrons are localized on Ti 3*d* orbitals and the oxygen vacancy sites.

S.G. Park, B. Magyari-Köpe, Y. Nishi, MRS. Symp. Proc. Vol. 1160, 2009.
S.G. Park, B. Magyari-Köpe, Y. Nishi, Proc. Nonvol. Mem. Work., Nov 2008.
S.G. Park, B. Magyari-Köpe, Y. Nishi, Phys. Rev B 82, 115109, 2010.

TiO_2: Multi Vacancy Filament Formation

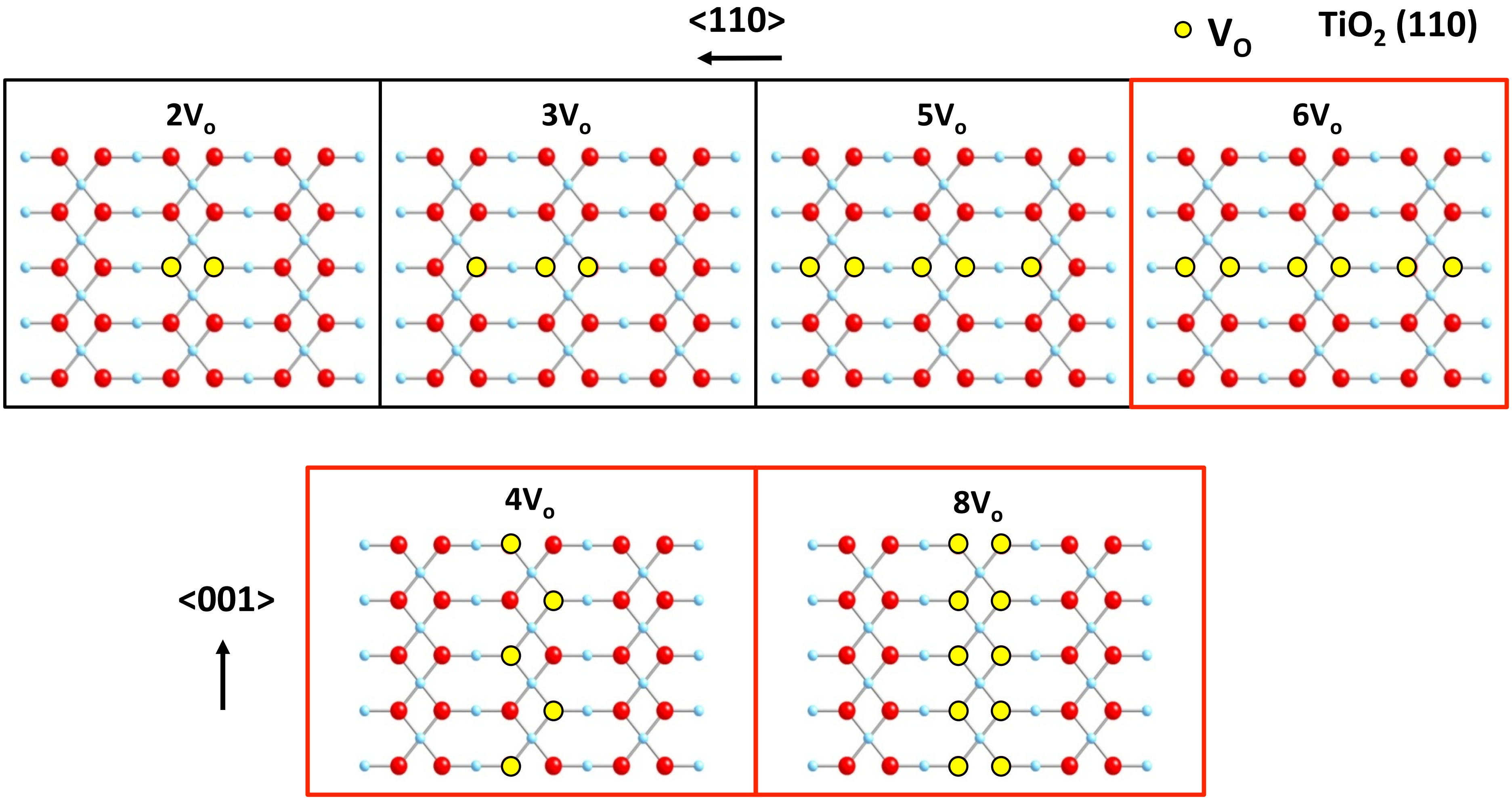

S.G. Park, B. Magyari-Köpe, Y. Nishi, Electron Dev. Lett. 32, 197, 2011.

TiO_2: Electron Delocalization Trends

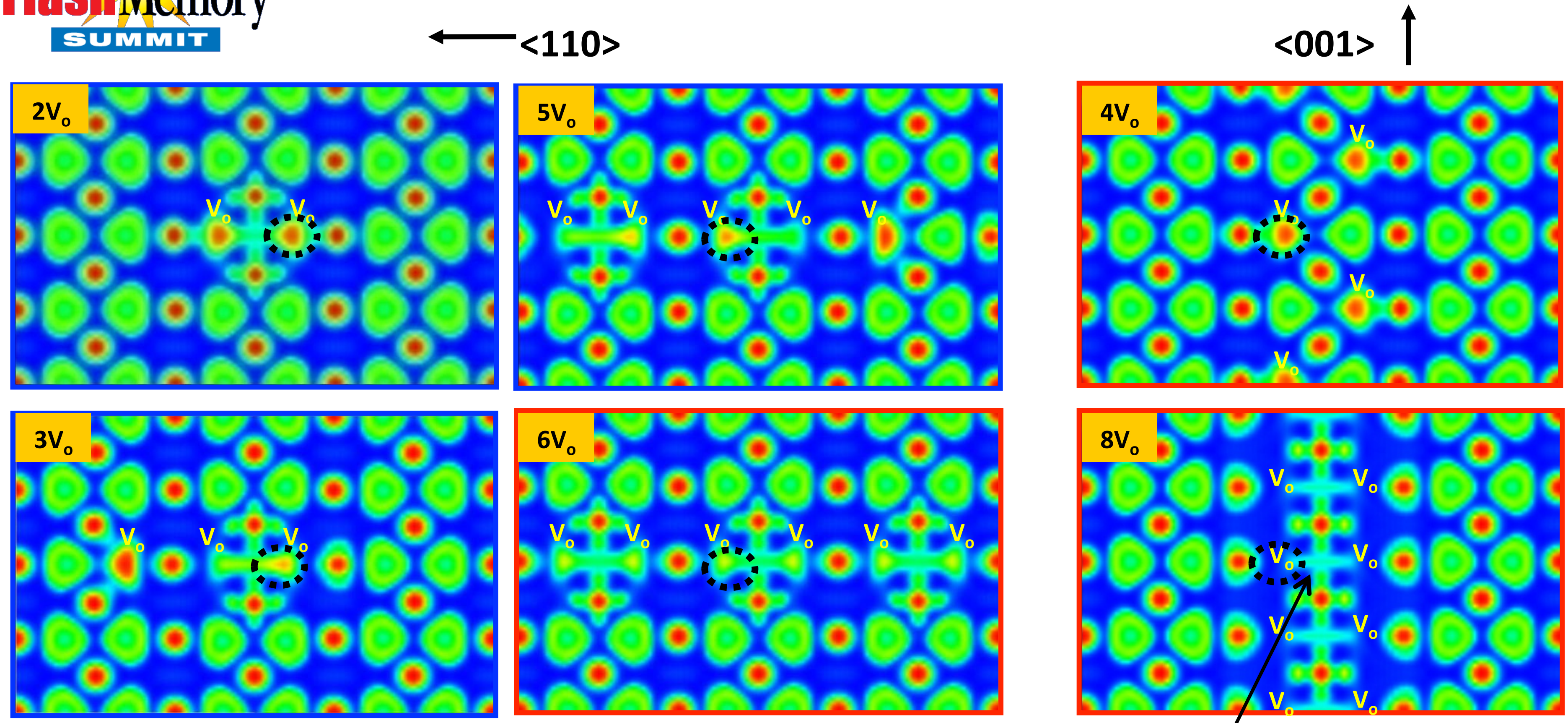

delocalized electrons

- **Electron delocalization trends** (electrons moving away from the oxygen vacancy sites) **are observed when the number of oxygen vacancy neighbors are increased.**

S.G. Park, B. Magyari-Köpe, Y. Nishi, Electron Dev. Lett. 32, 197, 2011.

TiO_2: Vacancy Filament Formation

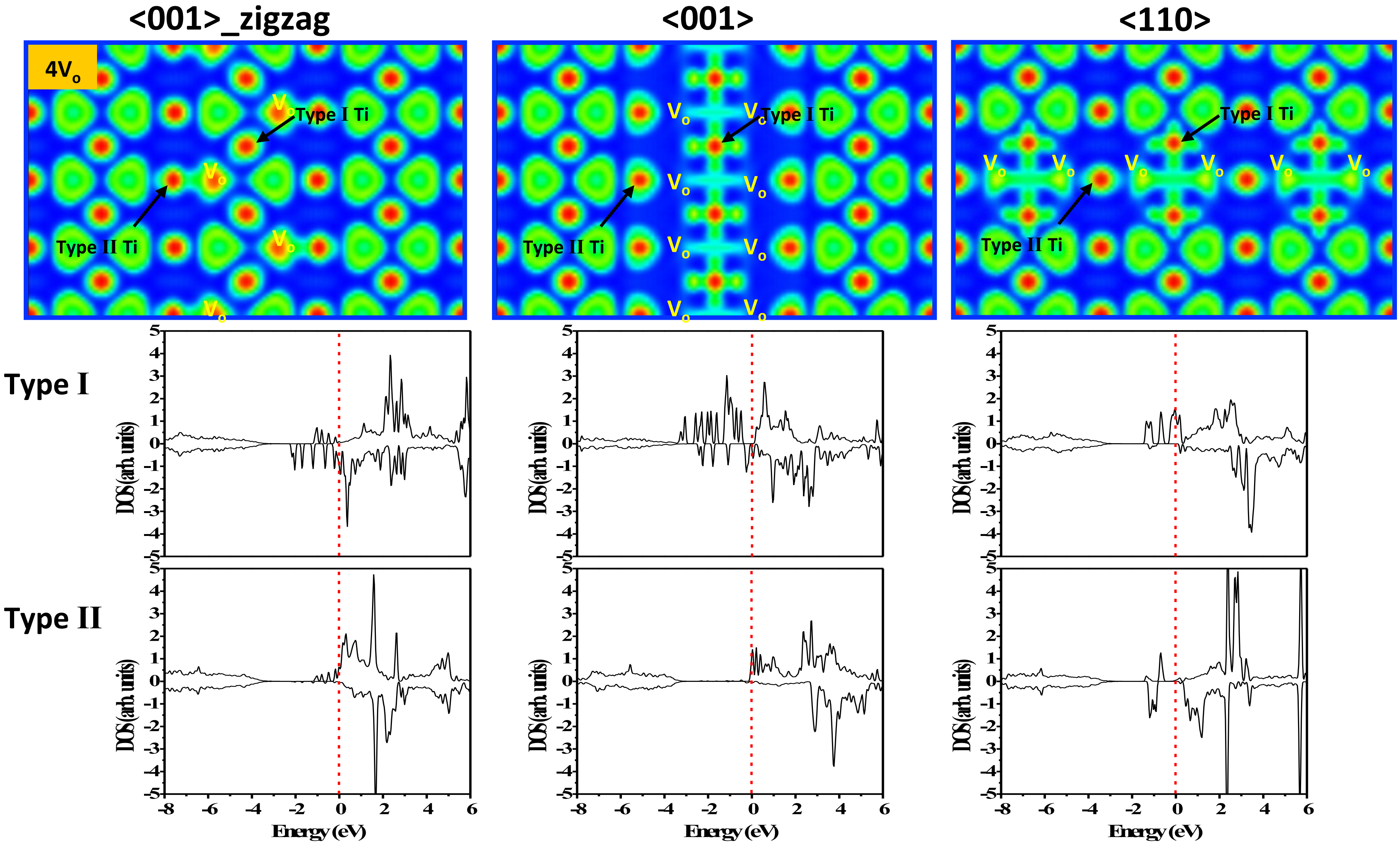

TiO_2: Randomly Distributed Vacancies

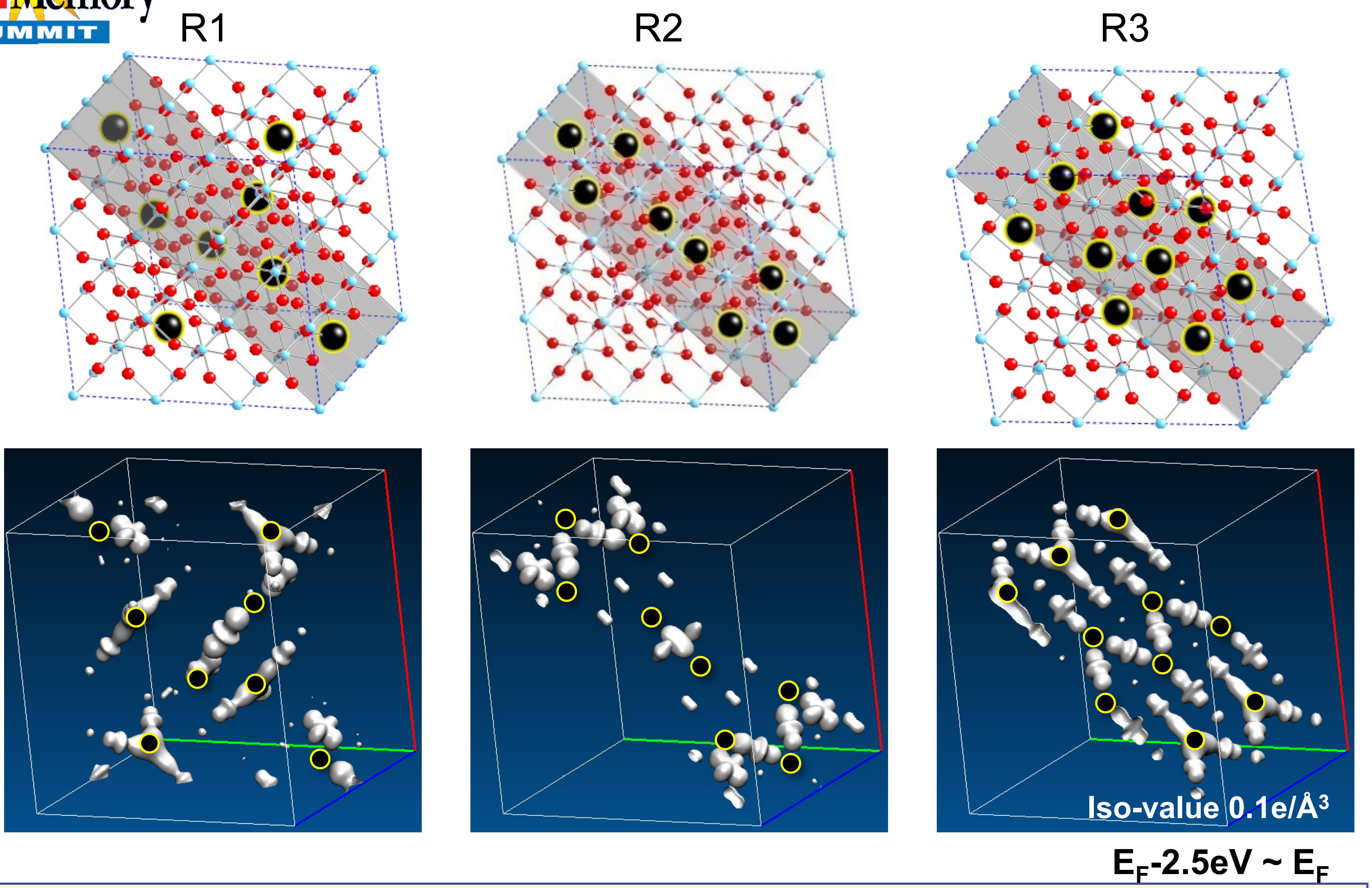

- **Electrons tend to localize around the oxygen vacancies in randomly distributed V_O configurations.**

TiO_2: Stability of Multi Vacancy Configurations

$$E_{vf} = E(TiO_{2-x}) - E(TiO_2) + n/2E(O_2)$$

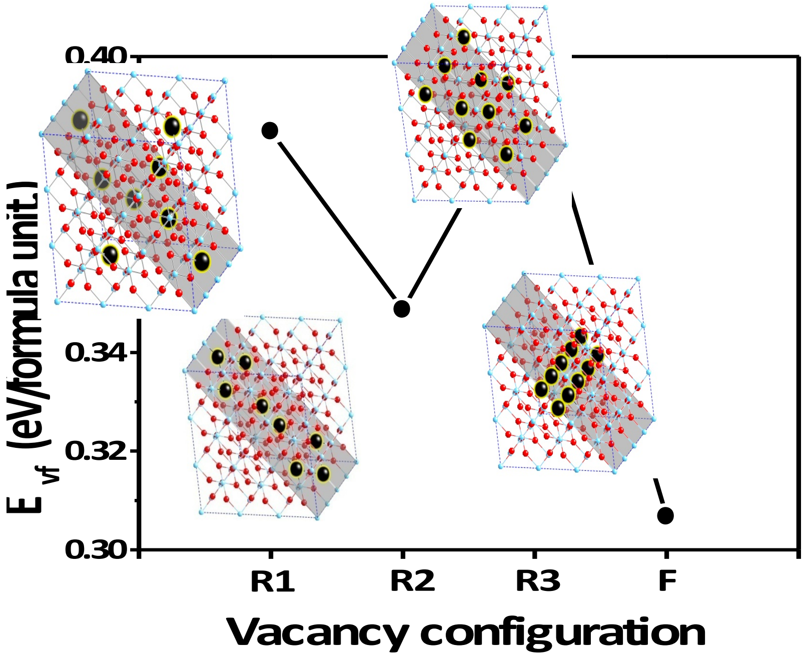

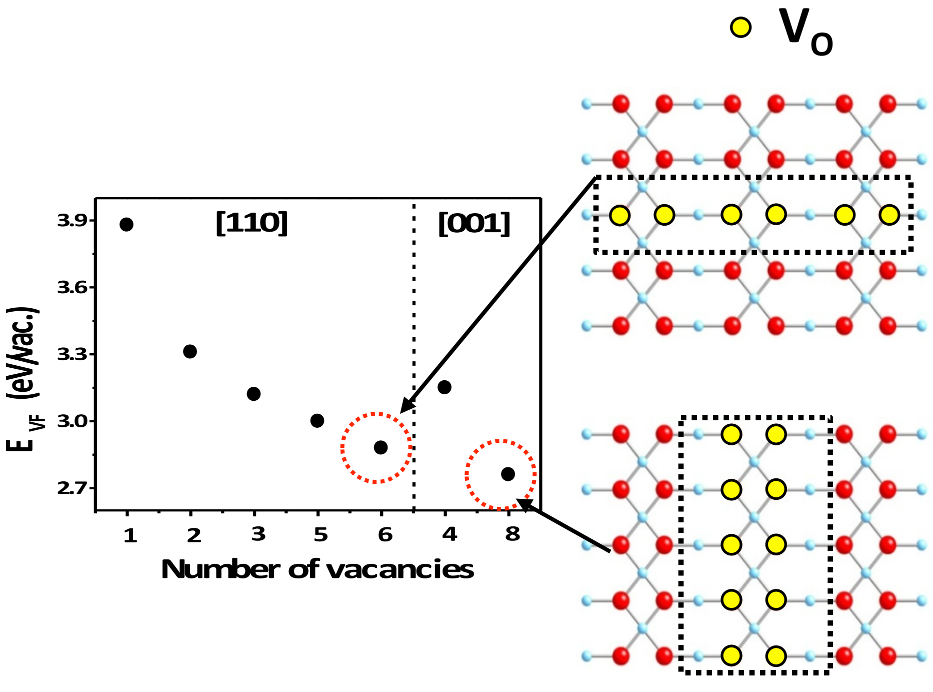

S.G. Park, B. Magyari-Köpe, Y. Nishi, Electron Dev. Lett. 32, 197, 2011.
B. Magyari-Köpe, M. Tendulkar, S.G. Park, H.D. Lee, Y. Nishi, Nanotechn. 22, 254029, 2011.
B. Magyari-Köpe, S. G. Park, H.D. Lee, Y. Nishi, J. Mater. Sci., 2012.

TiO_2: Conductive Filament Along [001]

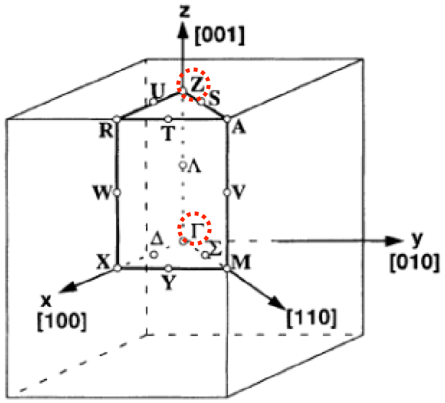

Γ : 0 0 0
Z : 0 0 1

(110)

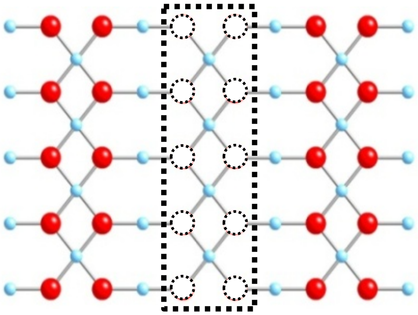

On –state

Partial charge density

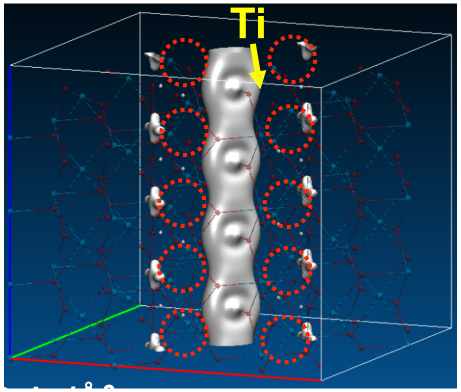

Spin up

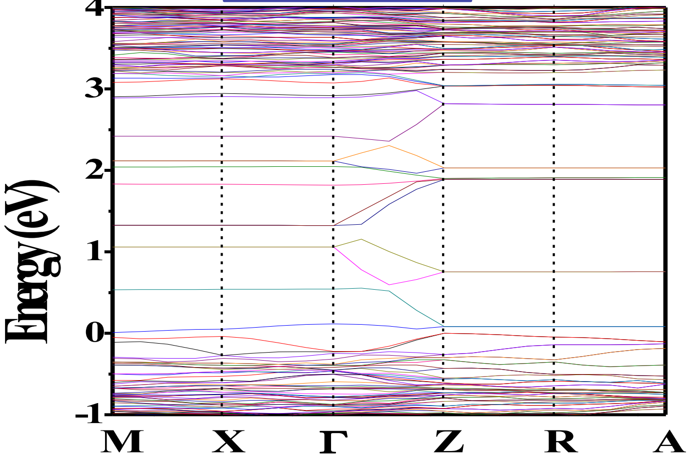

Spin down

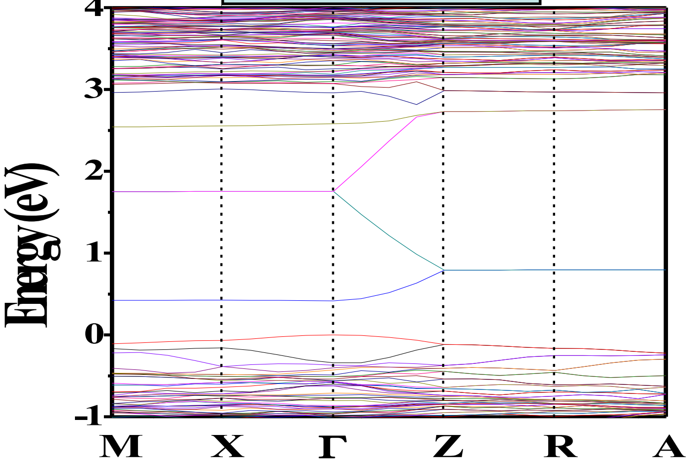

- **Electron motion is enhanced along the z-direction.**

S.G. Park, B. Magyari-Köpe, Y. Nishi, Tech. Digest VLSI Symp., 2011.

TiO$_2$: “ON” (LRS) to “OFF” (HRS) Transition

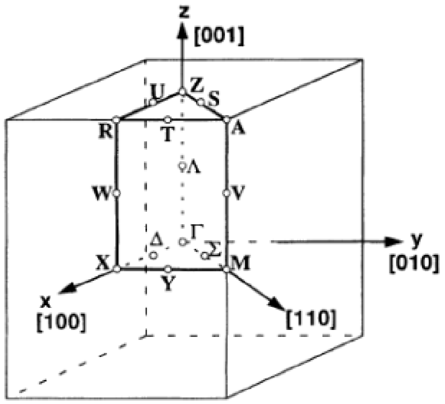

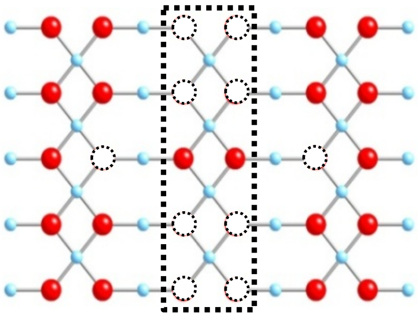

2V$_o$ off

Partial charge density

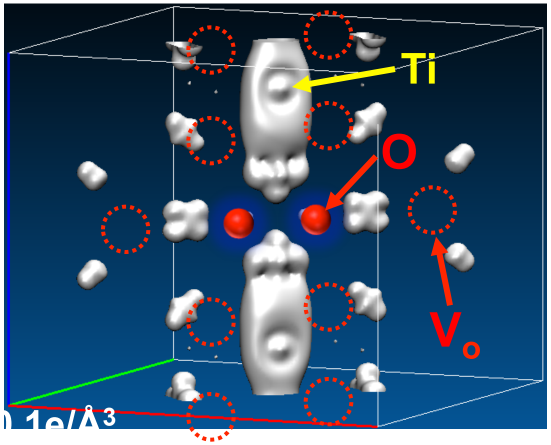

Spin up

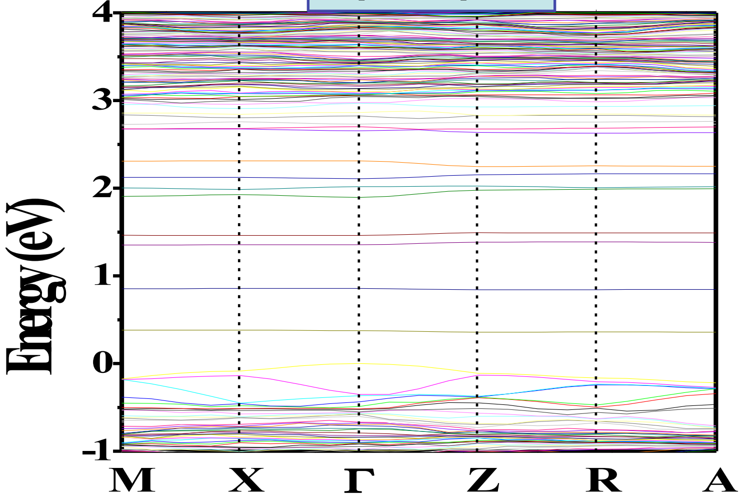

Spin down

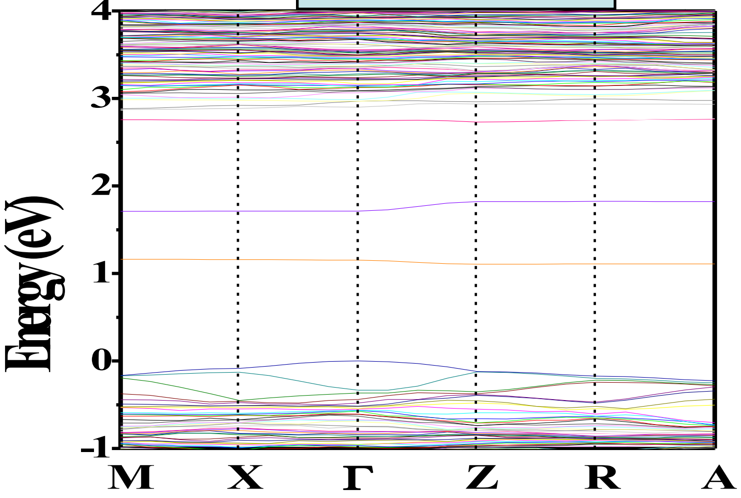

- **The energy levels become strongly localized → resistivity is increased.**

S.G. Park, B. Magyari-Köpe, Y. Nishi, Tech. Digest VLSI Symp., 2011.

TiO_2: Effect of H Doping on Conductive Paths

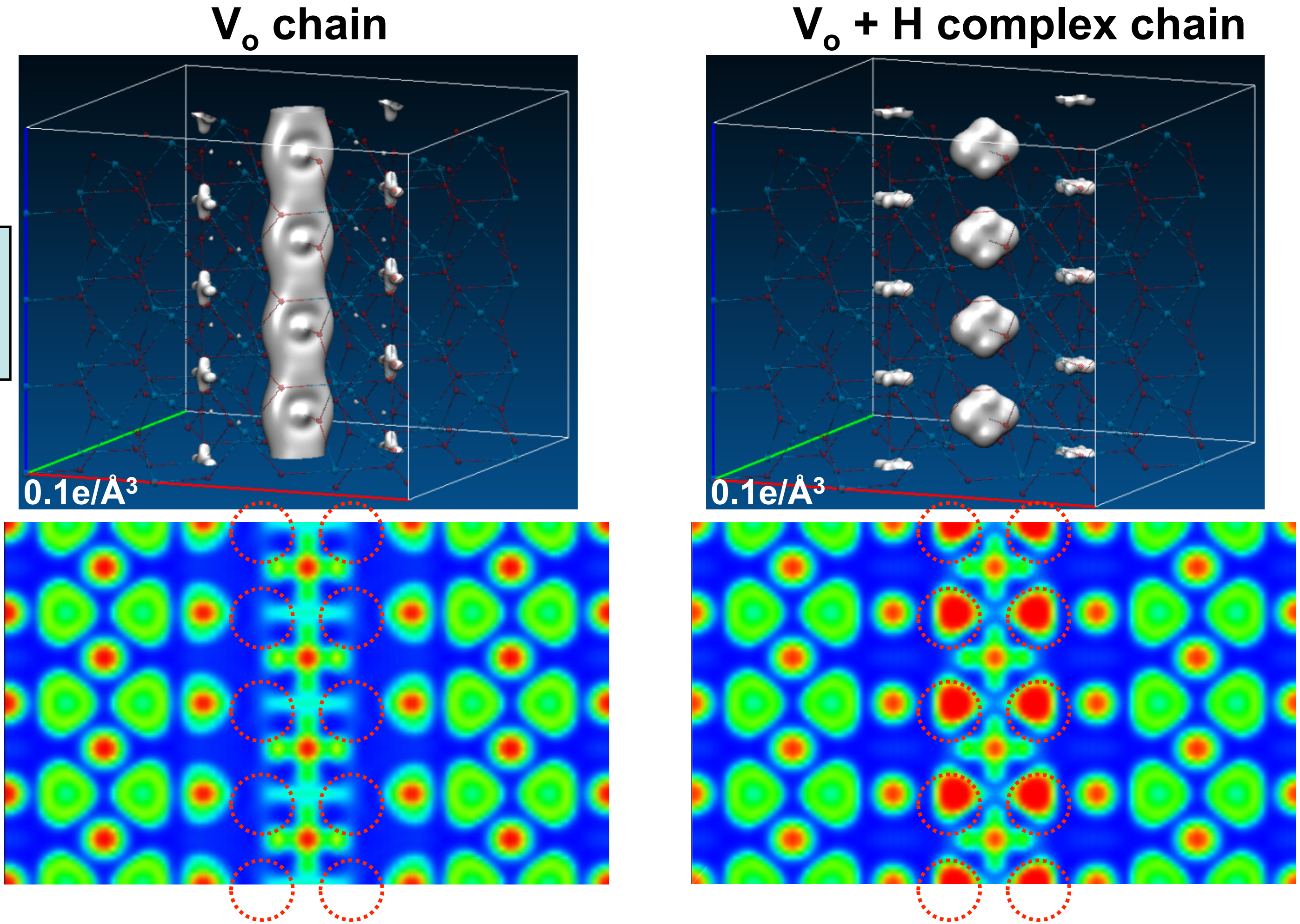

V_o chain

V_o + H complex chain

Partial Charge Density (defect states)

Electron Localization Function (ELF)

- **Hydrogen diffused into the vacancy site induces the rupture of the conductive channel by localizing electrons.**

S.G. Park, B. Magyari-Köpe, Y. Nishi, Tech. Digest VLSI Symp., 2011.

TiO_2: Role of Charge Trapping in Filament Destabilization

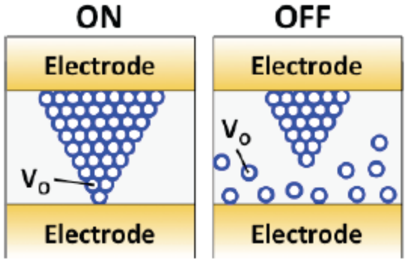

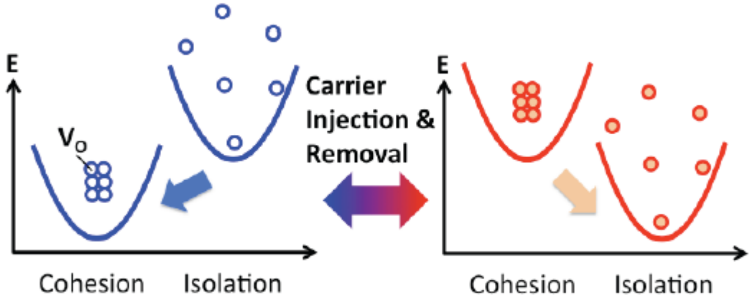

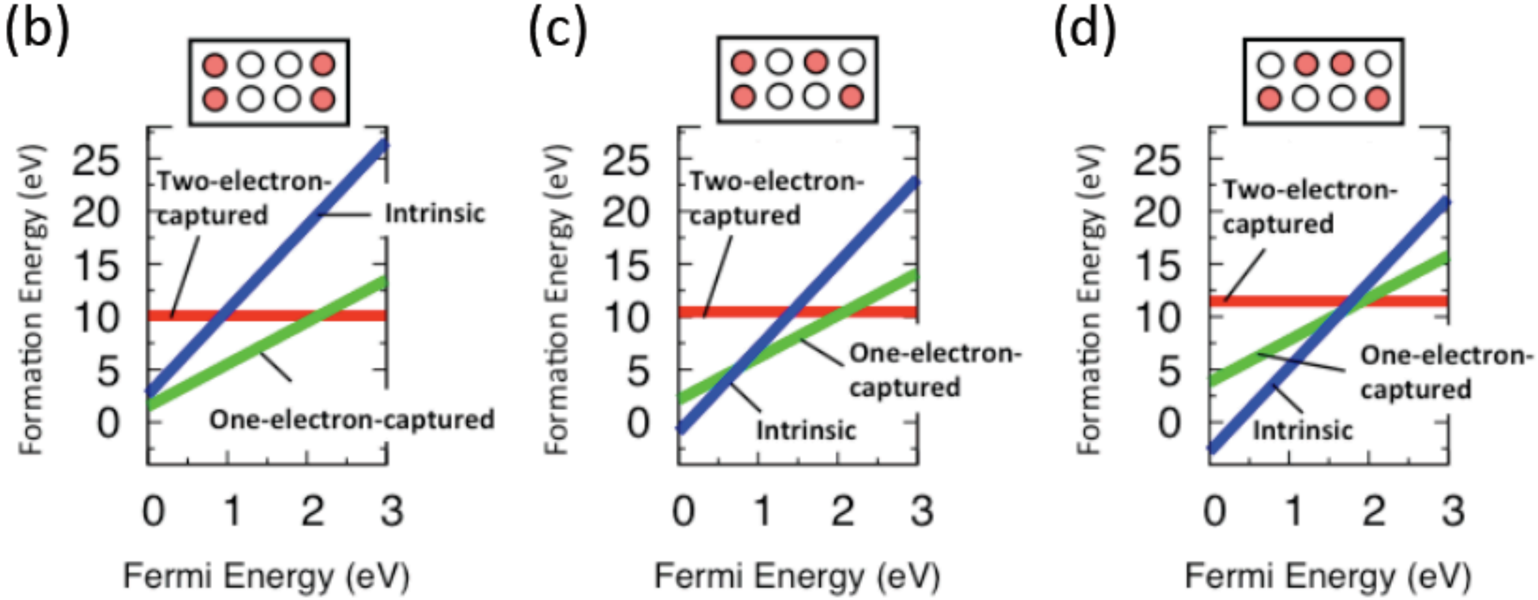

K.Kamiya, M.Y. Yang, S.G. Park, B. Magyari-Köpe, Y. Nishi, M. Niwa, and K. Shiraishi, APL 2012
L. Zhao, S.G. Park, B. Magyari-Köpe, et al., submitted 2012.

TiO_2: Schematics of the Proposed Switching Mechanism

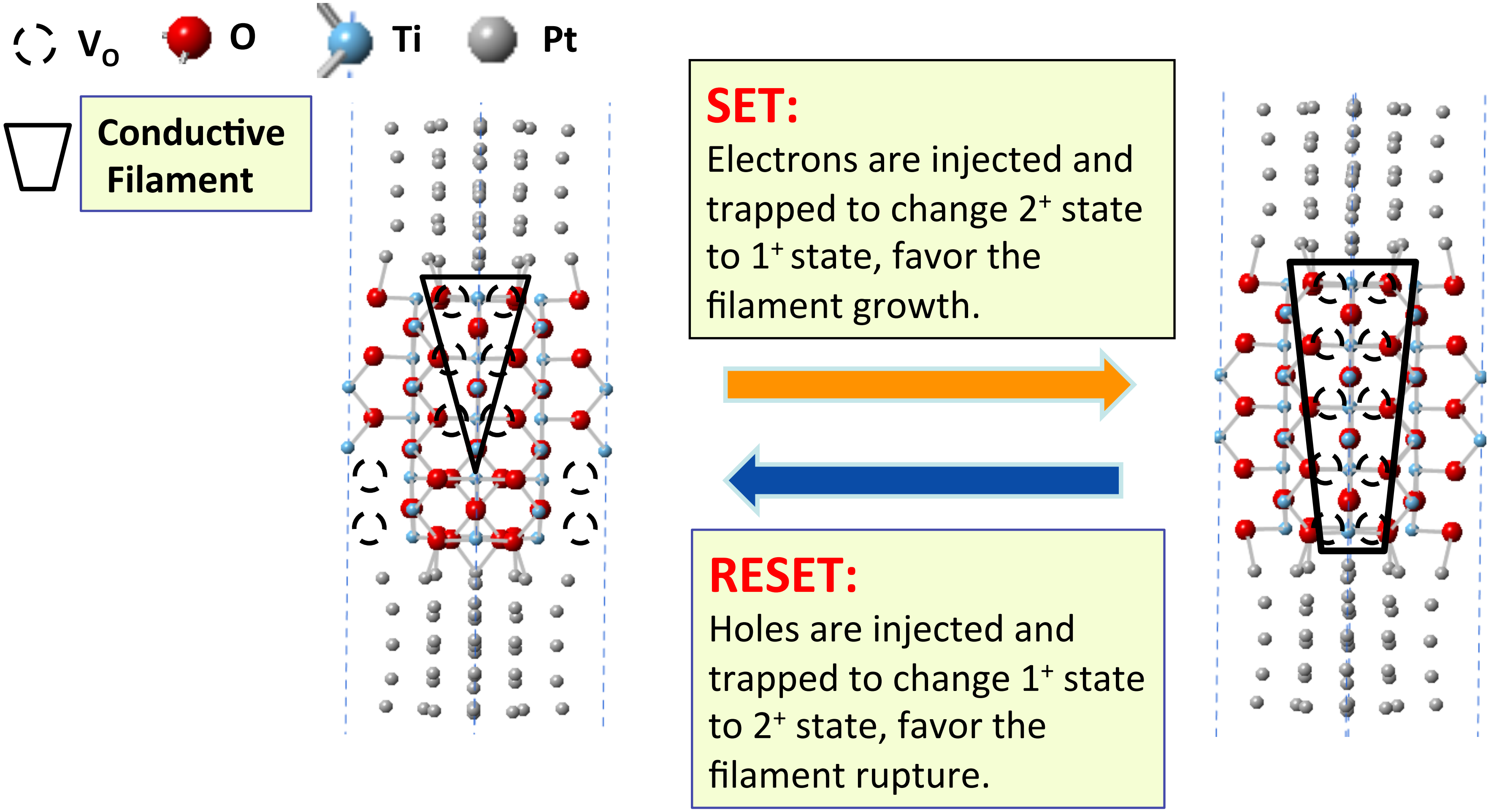

SET:
Electrons are injected and trapped to change 2^+ state to 1^+ state, favor the filament growth.

RESET:
Holes are injected and trapped to change 1^+ state to 2^+ state, favor the filament rupture.

L. Zhao, S.G. Park, B. Magyari-Köpe, et al., submitted 2012.

Macroscopic Switching Model

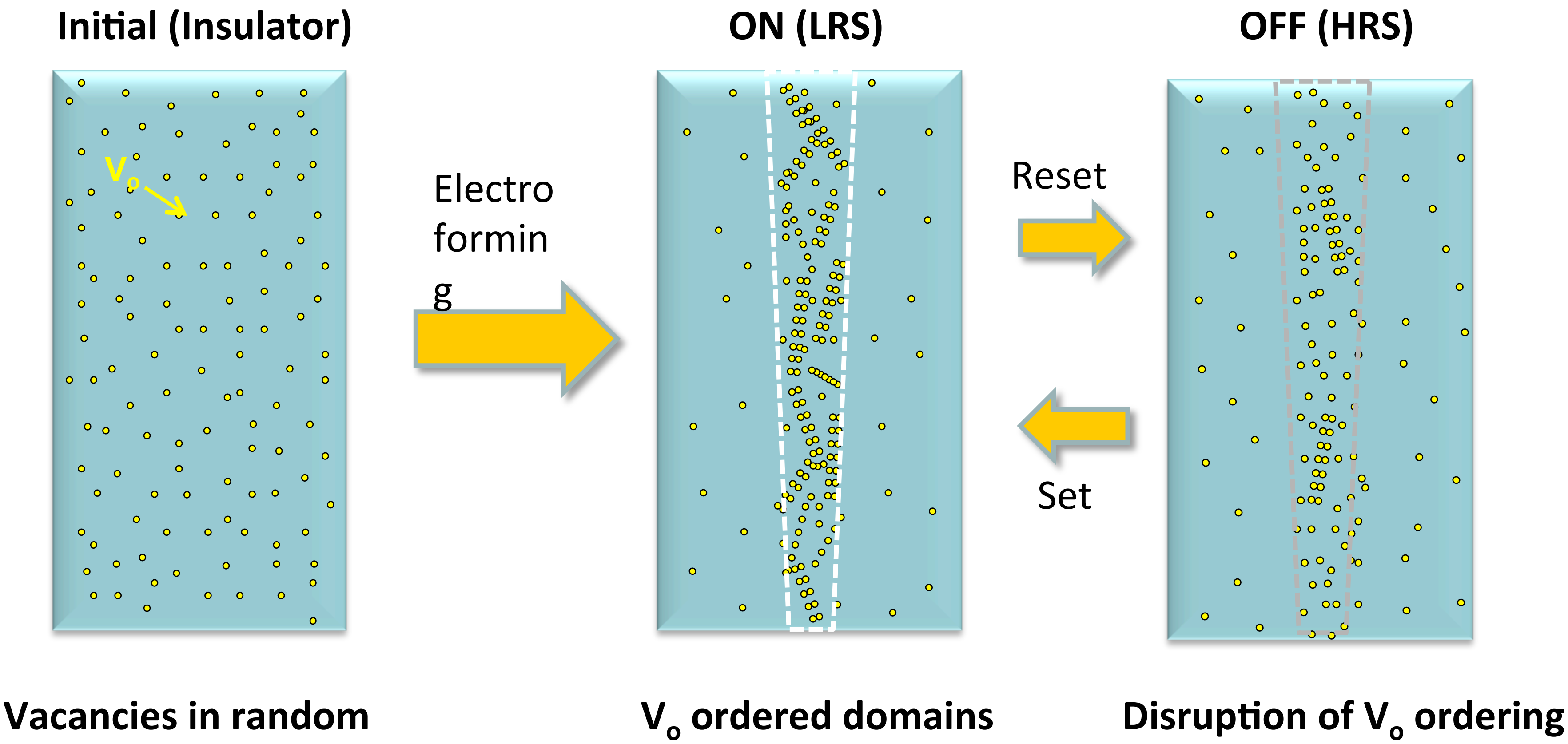

Initial (Insulator)

ON (LRS)

OFF (HRS)

Vacancies in random

V_o ordered domains

Disruption of V_o ordering

- **V_o concentration increases locally → V_o become ordered. (LRS)**
- **Thermal heating by high current density → V_o diffuse out (HRS)**

S.G. Park, B. Magyari-Köpe, Y. Nishi, Tech. Digest VLSI Symp., 2012.

Summary and Outlook

- **The multi-oxygen vacancy configuration is linked to the formation of a metallic filament.**

- **The chain like vacancy configurations may account for the higher conductivity observed in oxygen deficient TiO_2 and other transition metal oxides, i.e. NiO and HfO_2.**

- **Filament rupture can take place by oxygen or hydrogen at substitutional sites.**

- **Electron transport and interface effects also contribute to the formation of vacancy configurations – to be investigated.**